IET Microwaves, Antennas & Propagation

Research Article

Planar, compact ultra-wideband polarisation diversity antenna array

ISSN 1751-8725
Received on 15th October 2014
Accepted on 29th July 2015
doi: 10.1049/iet-map.2015.0371
www.ietdl.org

Muhammad Saeed Khan[1,2] ✉, Antonio-Daniele Capobianco[1], Aftab Naqvi[2], Bilal Ijaz[2], Sajid Asif[2], Benjamin D. Braaten[2]

[1]*Dipartimento di Ingegneria dell'Informazione, University of Padova, Via Gradenigo 6/b, 35131 Padova, Italy*
[2]*Department of Electrical and Computer Engineering, North Dakota State University, Fargo, ND 58102, USA*
✉ *E-mail: khan@dei.unipd.it*

Abstract: A new compact multiple-input multiple-output (MIMO) ultra-wideband (UWB) antenna array is presented. The antenna array initially consisted of two monopoles placed side by side at a distance of 4 mm. A strong mutual coupling was observed so the design was modified by rotating the second radiator at 90° at a distance of 1 mm. Wideband isolation is achieved by exploiting polarisation diversity of antenna elements. Simulation in HFSS and printed prototype results validate the high isolation, over 21 dB on the entire 2.5–12 GHz frequency range. A prototype was fabricated on a low loss substrate of Rogers TMM4 measuring 23×39.8 mm^2. To evaluate the diversity performance, the envelope correlation coefficient was calculated resulting below −20 dB, thus ensuring good diversity performance. The compactness of the proposed UWB-MIMO design is finally compared against alternative solutions already present in the literature.

1 Introduction

Mutual coupling between two antennas hinders the efficiency of designs for the applications of wireless communication, antenna arrays and multiple-input multiple-output (MIMO) systems. This is especially important in MIMO systems, where multiple antennas are placed in close proximity to each other in order to reduce the size of the designed device. Mutual coupling between these closely placed antennas should be minimised to attain high isolation between them and for the efficiency elevation of the individual antenna [1].

Besides the practice of shielding of antennas, from the electromagnetic compatibility point of view, antenna diversity is another potential candidate to alleviate the mutual coupling and enhance the system capacity. Polarisation diversity, where different antennas on a single prototype have a different sense of polarisation, is a well-known type of antenna diversity along with space/spatial and pattern diversity to simultaneously receive multiple transmissions [2].

Ultra-wideband (UWB) provides multiple simultaneous user channels, very low level of radiation, high data rate and reduced probability of detection, thus pushing more and more the interest of researchers in the area of wireless communication. Various types of UWB-MIMO antennas have been proposed earlier to reduce the size and decrease the mutual coupling among the antenna elements. The work presented in [3] uses an annular slot to achieve pattern diversity, which ensures an isolation of better than 15 dB between ports but it has a larger size (80×80 mm^2). In [4], the isolation of better than 20 dB is achieved by polarisation diversity but still the size is large (56×56 mm^2). A compact size (25×48 mm^2) antenna array with slots in the radiators is reported in [5] but its bandwidth range is 80% of the UWB frequency range. In [6–12], various decoupling structures or stubs were employed between two radiators to enhance the isolation. Perpendicular feeding directions were used in [13–16] to achieve the pattern and polarisation diversity. In [17], parasitic digitated decoupling structure and in [18], parasitic elements have been used to improve the isolation. Another technique involves negative waveguide material to reduce the mutual coupling [19]. Among the aforementioned designs, some were not able to operate in the entire UWB band allocated by the Federal Communications Commission (FCC) [5, 9, 16]. For those designs which could cover the entire UWB range [3, 4, 6–8, 10–15, 17], some were not compact enough for portable devices [3, 13, 15]. For example, in [3, 15], the sizes of the MIMO antennas were 80×80 mm^2. In [13], a complicated three-dimensional (3D) feeding network with a large volume was required. For the rest of these antennas, the smallest size was presented in [12], which is $26 \times 40 = 1040$ mm^2. An isolation of more than 15 dB is achieved by placing two radiators perpendicularly to each other and also inserting stubs on the ground plane.

In this paper, the linear UWB-MIMO antenna array shown in Figs. 1*a* and *c* with two radiating elements is used as initial step of our design. Elements are first placed side by side with an edge separation of 4 mm. A strong mutual coupling among the antenna elements was observed. Finally, these radiators are placed at 90° to each other to realise the polarisation diversity and guarantee the high isolation. The proposed antenna array 2 has compact size $23 \times 39.8 = 915.4$ mm^2, about 13% smaller as compared with the antenna presented in the literature [12]. Simulation in HFSS [20] and measurement results in terms of *S*-parameters and radiation patterns of antenna prototypes are presented. Orthogonal polarisation of antenna elements is verified by plotting surface current and by calculating the difference between θ and φ components of E-field. Finally, diversity analysis has been carried out to show the effectiveness of the proposed design.

2 Antenna design

The geometry of proposed antenna system with overall dimensions is presented in Fig. 1. A monopole radiator with straight edges and arced feeding section, having partial ground plane, was designed and characterised with numerical simulation using commercially available software, HFSS [20]. The second monopole was then placed beside the first one at a distance of 4 mm from the edge as shown in Fig. 1*a*. An impedance mismatch was observed in the

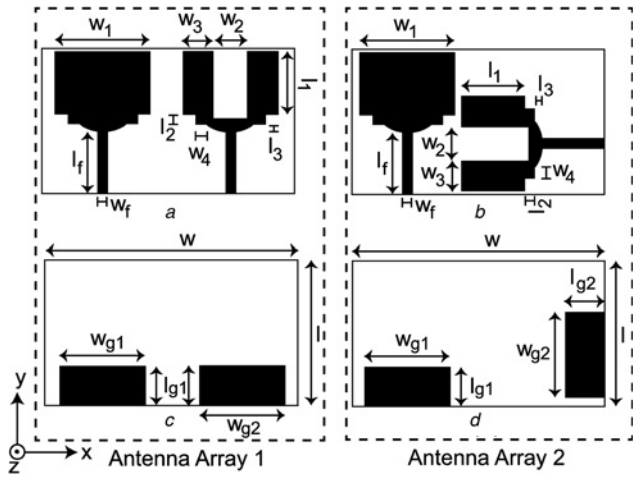

Fig. 1 *Layout of the proposed UWB-MIMO antenna array with overall dimensions: $w = 39.8$ mm, $l = 23$ mm, $w_1 = 15$ mm, $w_2 = 5$ mm, $w_3 = 5$ mm, $w_4 = 2.25$ mm, $l_1 = 10$ mm, $l_2 = 1.5$ mm, $l_3 = 1.1$ mm, $w_f = 1.5$ mm, $l_f = 9.85$ mm, $w_{g1} = w_{g2} = 13.5$ mm, $l_{g1} = l_{g2} = 6.25$ mm*

lower band of antenna array 1, so a u-shaped slot was inserted in the radiator 2 to match the wideband characteristics [21]. The coupling between the elements was high. So keeping the same substrate and radiator dimensions, a second radiator was placed at 90° to the first radiator resulting in antenna array 2 as shown in Figs. 1*b* and *d*, to exploit the polarisation diversity, which results in the high isolation. The *S*-parameters of antenna array 1 are compared with antenna array 2 as shown in Figs. 2 and 3, respectively. The improvement in the *S*-parameter results of antenna array 2 can be seen. The isolation among the elements was improved more than 10 dB when polarisation diversity was exploited.

3 Working principle of antenna array 2

To demonstrate the working principle of proposed antenna array 2, the simulated surface current distribution at 7.1 GHz is presented in Fig. 4.

Fig. 4*a* shows the surface current vector when port 2 is terminated with a 50 Ω matched load and port 1 is excited and Fig. 4*b* shows the current vector port 1 is terminated while port 2 is excited. It is observed from the plot that when port 2 is matched, the current vectors are aligned with the *y*-axis, which leads to an E-field linear polarisation [2]; and similarly when port 1 is matched, the current vectors are aligned with the *x*-axis, which leads to a linear *x*-polarisation. The colours representing the current distribution vary from dark grey (weak current density) to grey, and black (strong current density). Similarly, the surface current vectors on antenna array 1 are also plotted. It can be observed that current vectors are aligned in the *y*-direction on both antenna elements, when port 1 or port 2 is excited in Figs. 4*c* and *d* which leads to strong coupling. A similar behaviour of the currents in Figs. 4*c* and *d* was observed when two identical elements (without slots) were placed side by side.

To elaborate further the polarisation diversity of antenna array 2, the simulated power level difference in the patterns of the two polarisation components [θ component (dB) minus φ component (dB)] in the *x*–*z* and *y*–*z* planes is calculated as explained in [16]. In [16], the polarisation diversity is also exploited by placing two antenna elements at 90° to each other, but it also uses slots and tapered geometry on the ground plane to achieve 40% of the UWB bandwidth range. In Table 1, it is shown that the purity of polarisation can be kept high for antenna element 1 in both planes, while polarisation of antenna elements 2 is smaller than antenna element 1; this is due to the u-shaped slot which decreases the power level of antenna element 2. The opposite sign of polarity in power level difference shows that the polarisations for two elements are quite orthogonal to each other. On the basis of this mechanism, good impedance bandwidth and isolation can be achieved over a wide bandwidth, despite that the two elements are placed very close to each other (i.e. the distance between two elements in antenna array 2 is only 1 mm).

4 Fabrication and measurement

The proposed antenna was printed on a low-loss Roger TMM4 laminate (thickness 1.524 mm, dielectric constant 4.5 and a loss tangent 0.002) with a spacing of 1 mm as shown in Fig. 5.

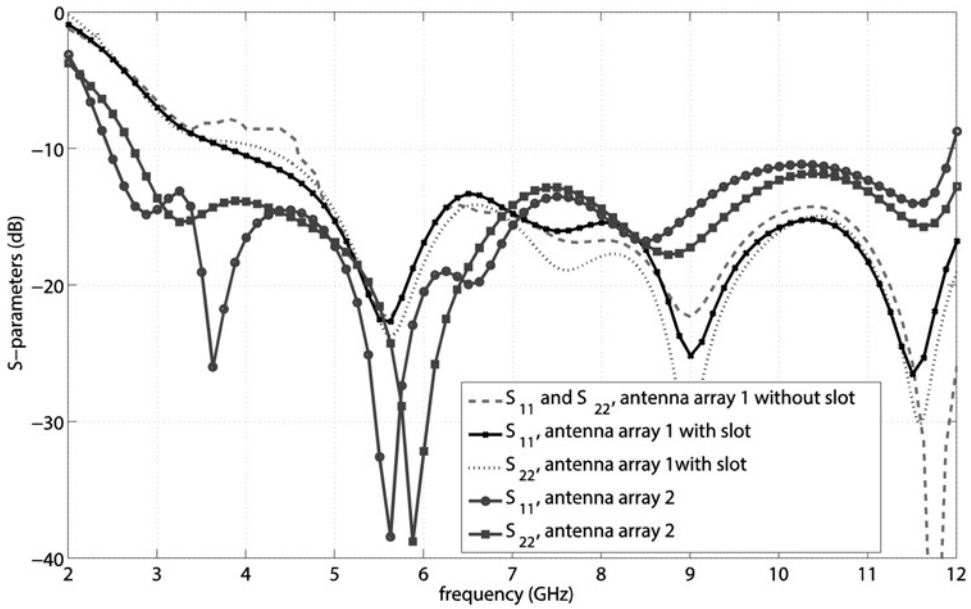

Fig. 2 *Comparison of simulated S-parameters of antenna array 2 with antenna array 1*

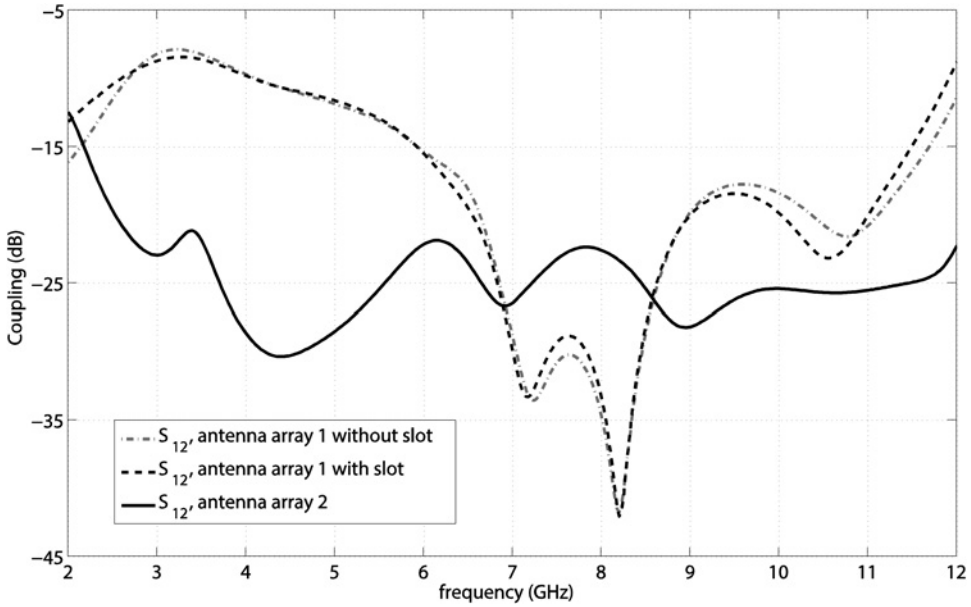

Fig. 3 *Comparison of mutual coupling of antenna array 2 with antenna array 1*

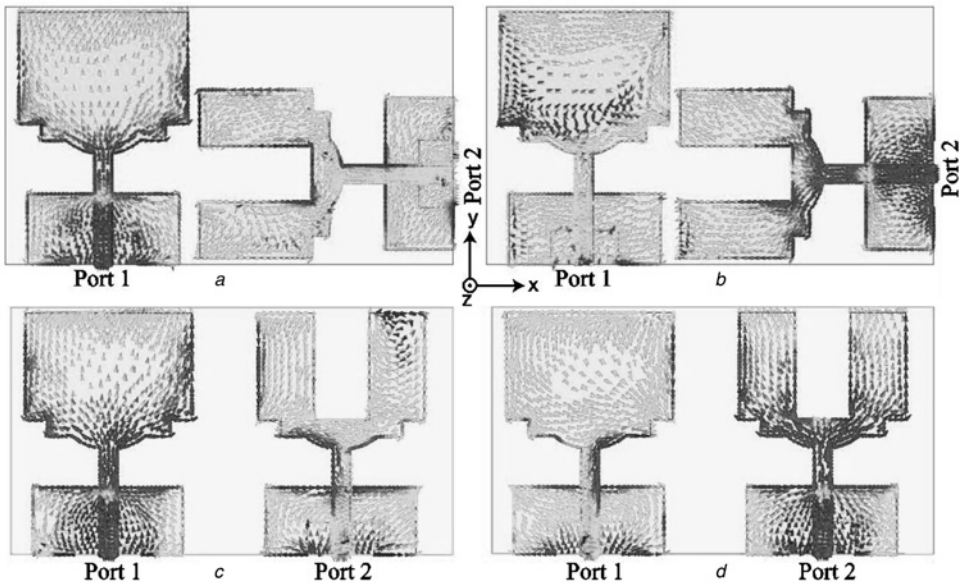

Fig. 4 *Surface current distribution at 7.1 GHz*

a Port 1 is excited
b Port 2 is excited
c Port 1 is excited
d Port 2 is excited

Table 1 Power level difference in the selected planes (θ component peak value minus φ component peak value)

Frequency, GHz	*y–z* plane		*x–z* plane	
	Radiator 1, dB	Radiator 2, dB	Radiator 1, dB	Radiator 2, dB
2.5	18.2	−10.2	−17.5	10.7
3.5	18.5	−09.8	−16.3	12.5
4.5	19.2	−11.3	−15.4	13.3
5.5	19.7	−13.5	−17.2	12.7
6.5	18.2	−14.5	−16.2	15.4
7.5	18.7	−10.2	−15.4	14.8
8.5	16.2	−08.5	−12.4	14.9
9.5	16.6	−11.5	−13.5	13.7
10.5	15.9	−10.2	−14.3	14.3
11.5	16.3	−12.3	−13.9	15.2

Fig. 5 *Photograph of the proposed antenna array 2 prototype*

a Top layer
b Bottom layer

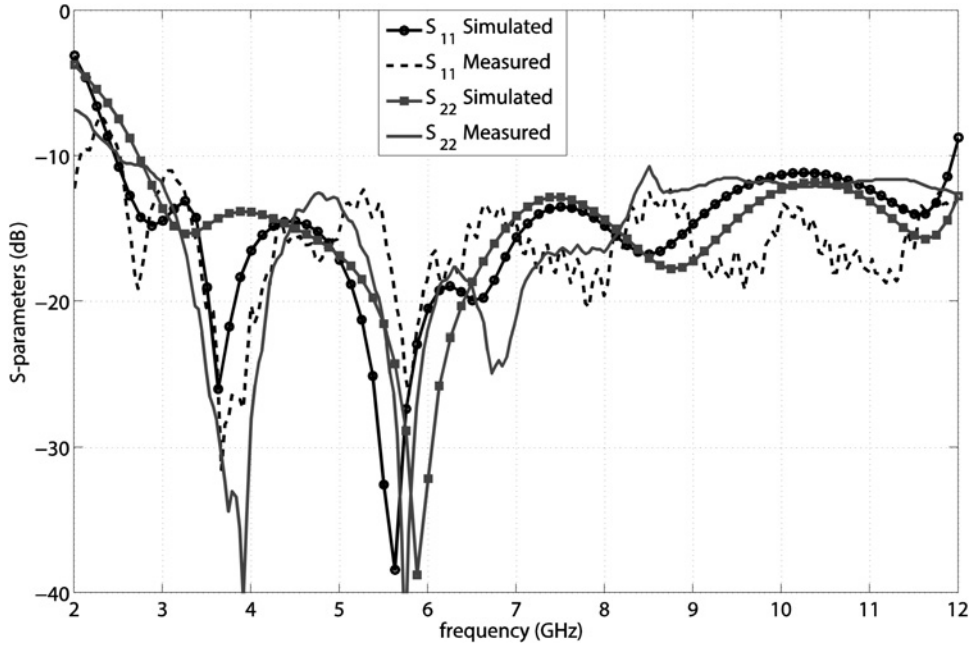

Fig. 6 *Simulated and measured S-parameters of the proposed antenna array 2*

4.1 Scattering parameters

The measurements were taken using a two port Agilent N5242A PNA-X network analyser. Simulated scattering parameters are plotted along with the measured scattering parameters in Figs. 6 and 7. A good agreement between simulated and measured results has been observed. Slight variations between results are attributed to dispersive properties of substrate and fabrication imperfections. The measured results in Fig. 6 show that port 1 has a bandwidth from 2.3 to 12 GHz for $S_{11} < -10$ dB, while port 2 has a bandwidth from 2.5 to 12 GHz for $S_{22} < -10$ dB. Along with the impedance matching, mutual coupling of <-15 dB is considered to be adequate for good performance. The simulated S_{21} (mutual coupling) is plotted along with measured mutual coupling in Fig. 7. Mutual coupling of <-21 dB in both simulated and measured results throughout the UWB range ensures that the proposed antenna array is well suited for MIMO operations across the UWB spectrum.

4.2 Radiation patterns

The radiation patterns of our proposed UWB-MIMO antennas are measured in an anechoic chamber in the *x*–*z* and *y*–*z* planes and shown in Fig. 8. When the pattern of one element is measured, the other is terminated with a 50 Ω matched load. The behaviour of radiation patterns of radiator 1 in the *x*–*z* plane is almost similar to radiator 2 in the *y*–*z* plane except at some middle frequencies due to the u-shaped slot in radiator 2. Similarly, the patterns of radiator 1 in the *y*–*z* plane are similar to the patterns of radiator 2 in the *x*–*z* plane except few variations. It can also be seen that the patterns (co-polarised components) are omnidirectional in the *x*–*z* plane

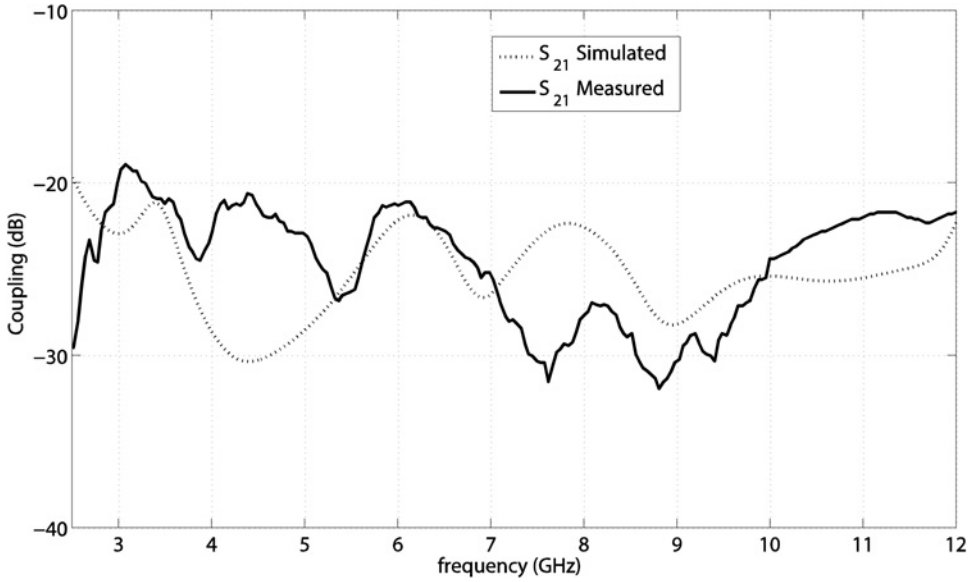

Fig. 7 *Simulated and measured mutual coupling of the proposed antenna array 2*

IET Microw. Antennas Propag., 2015, Vol. 9, Iss. 15, pp. 1761–1768

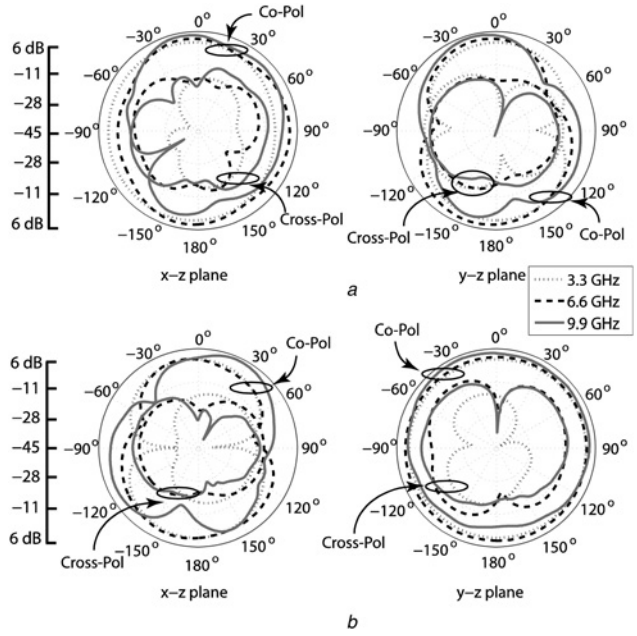

Fig. 8 *Measured radiation patterns of the proposed antenna array 2 at 3.3, 6.6 and 9.9 GHz*

a When port 1 is excited
b When port 2 is excited

(*H*-plane) for radiator 1 and in the *y*–*z* plane (*H*-plane) for radiator 2, which is similar to typical monopole antennas. However, the patterns (co-polarised components) deviate from dumb-bell shaped at higher frequencies and do not have a null in the *y*–*z* plane (*E*-plane) for radiator 1 and *x*–*z* plane (*E*-plane) for radiator 2, which are different from those of typical monopole antennas. This is due to the very small spacing between the two antenna elements, which affects the patterns of the other element. Since the direct feed radiation patterns are somewhat blocked (between 0° and 180°) by the other branch and subminature version A (SMA) terminated with a 50 Ω load, the known effects of increasing side lobes and nulls is seen at higher frequency [2].

4.3 Gain and efficiency

The realised peak gains of the proposed antenna array 2 with ports 1 or 2 excited are shown in Fig. 9. It can be seen that measured peak gains agree quite well with simulated peak gains. The measured peak gains vary from 2.4 to 5.1 dBi for port 1 across the frequency range from 2.5 to 12 GHz, while gain variations for port 2 are from 2.5 to 5.3 dBi. The simulated total efficiency of the proposed antenna array 2 is plotted in Fig. 10 and it is also compared with the total efficiency of antenna array 1. The comparison shows that the total efficiency of antenna array 2 is better than antenna array 1. The total efficiency of antenna array 2 remains above 82% across the whole frequency band while in antenna array 1 it drops to 55% at some frequencies due to strong mutual coupling.

5 Diversity analysis

Two or more different radiation patterns are employed to mitigate the effects of multipath in the pattern diversity hence to reduce the probability of fading occurring simultaneously to all patterns at the same frequency. In the proposed antenna array, two elements are placed at 90° to each other. This configuration results in two different radiation patterns in a plane as shown in Fig. 8. When compared, Fig. 8*b* has a null around −15° while at that point Fig. 8*d* has a +ve gain. Similarly, Fig. 8*d* has a gain of −22 dB around 10° while Fig. 8*b* has a +ve gain in that direction. These types of complementary patterns can also be observed in the *x*–*z* plane shown in Figs. 8*a* and *c* (i.e. a null in the radiation pattern of one radiating element is covered by the radiation pattern of other radiating element). Since the patterns of the radiating elements are uncorrelated, the basic requirement of pattern diversity is fulfilled. The correlation ρ_e, between antenna elements can be calculated using the 3D radiation patterns as calculated in [17]. The envelope correlation coefficient (ECC) for isotropic, indoor and outdoor environments has been calculated and shown in Fig. 11. The ECC values are <0.55 over the complete spectrum

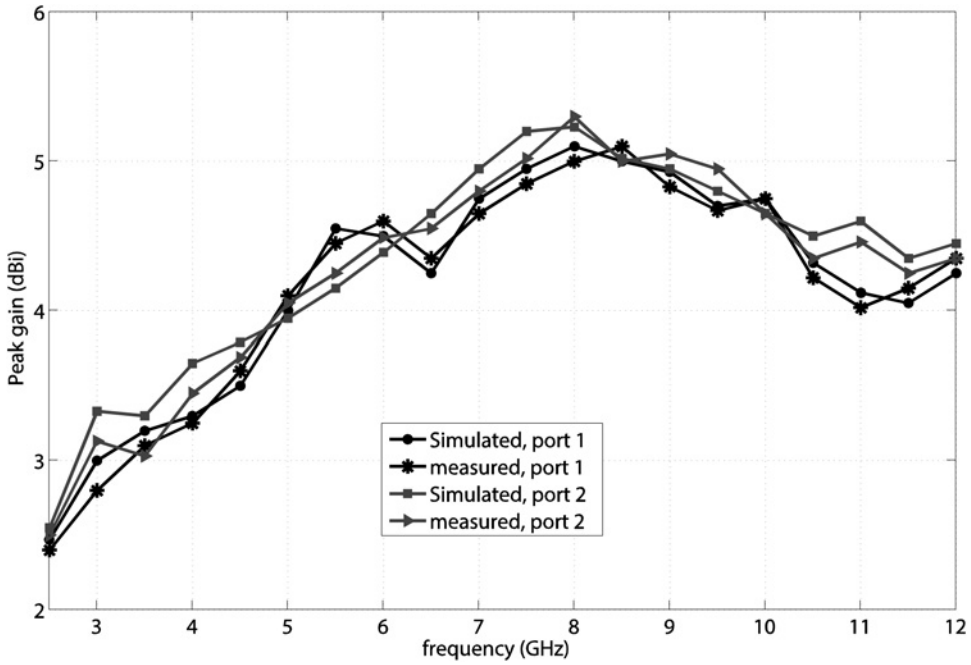

Fig. 9 *Simulated and measured peak gain of antenna array 2*

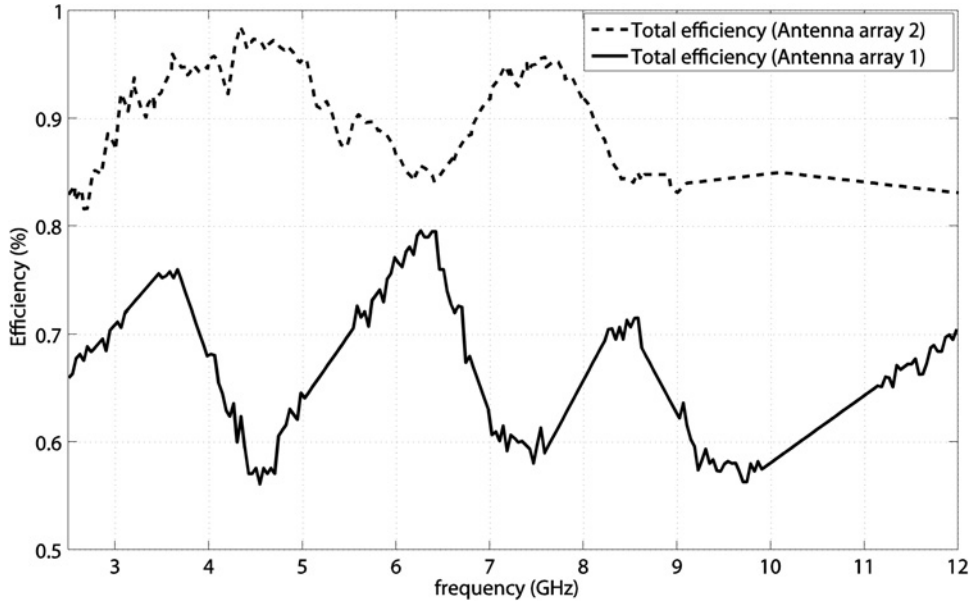

Fig. 10 *Comparison of the simulated total efficiency of antenna array 2 with antenna array 1*

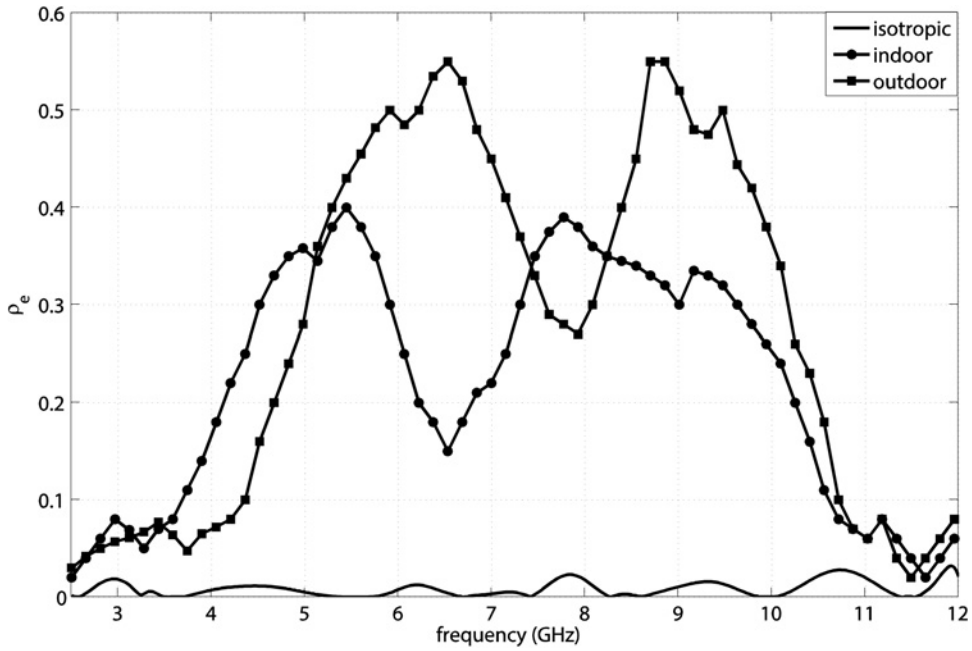

Fig. 11 *Simulated ECC of antenna array 2 for isotropic, indoor and outdoor environments*

in all three environments ensuring good diversity performance of the proposed antenna array 2.

The ECC ρ_s can also be calculated from the *S*-parameters according to eqn. 1 in [2]. The numerical calculated value of the proposed UWB diversity antenna array 2 in this paper from the measured *S*-parameters is below −20 dB across the entire bandwidth, as shown in Fig. 12. The ECC value of the proposed antenna array 2 has also been compared with antenna array 1. The ECC value of the proposed antenna array 2 is 13 dB less than antenna array 1. Since the ECC value of our proposed antenna system is very low and comparable to the existing literature, it guarantees that the proposed antenna array is well suited for MIMO/diversity applications.

Finally, to check the time-domain performance of the proposed antenna array 2, a pair of identical antenna arrays were placed in front of each other at a distance of 13 cm and the group delay was measured. In this set-up, one port of each array was terminated with a 50 Ω matched load. The group delay variations were <350 ps over the complete spectrum as shown in Fig. 13.

Finally, a comparison of the proposed work with the existing literature is presented in Table 2. It shows that the proposed design attains better results in mocst categories and comparable results in the remainder.

6 Conclusion

A compact printed UWB polarisation diversity antenna array with two radiating elements has been proposed. These monopole radiators are placed side by side and high isolation among the

IET Microw. Antennas Propag., 2015, Vol. 9, Iss. 15, pp. 1761–1768

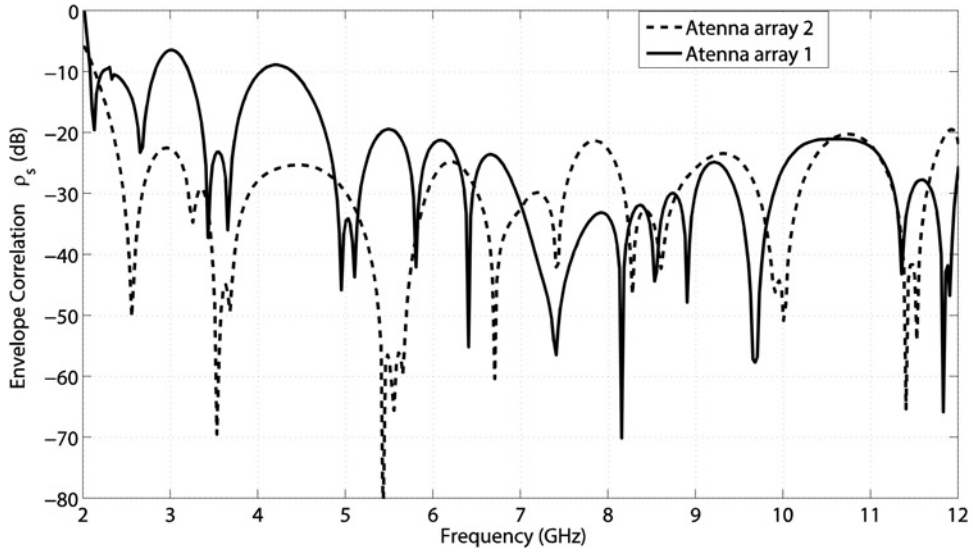

Fig. 12 *Comparison of numerically calculated ECC from measured S-parameters of antenna array 2 with simulated S-parameters of antenna array 1*

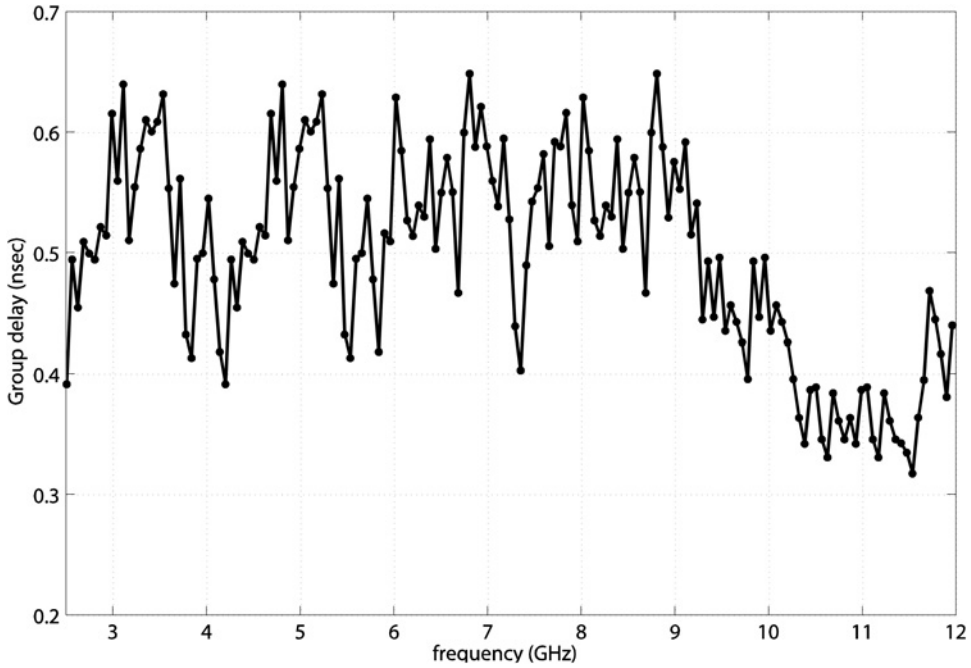

Fig. 13 *Measured group delay of the proposed antenna array 2*

Table 2 Comparison of the proposed antenna array with existing literature

Published literature	Antenna size, mm^2	Total band, GHz	Overall isolation, dB	Gain variation, dBi/total efficiency, %	ECC using *S*-parameters	ECC using radiation patterns
Gallo *et al.* [3]	80 × 80	3–12	>15	NA/60	<0.1	NA
Adamiuk *et al.* [13]	40 × 40	3.1–10.6	>20	4/NA	NA	NA
Daviu *et al.* [15]	80 × 80	3–12	>15	NA/NA	<0.02	NA
Khan *et al.* [17]	33 × 45.5	3.1–10.6	>20	2.3/85	<0.05	<0.6
Proposed	23 × 39.5	2.5–12	>21	2.8/82	<−20 dB	<0.55

antenna elements was observed. Later on, monopole radiators were placed at 90° to each other at a distance of 1 mm so that the antenna array dimensions were reduced to $23 \times 39.8\ mm^2$. The measured bandwidth for port 1 was from 2.3 to 12 GHz and for port 2 was from 2.5 to 12 GHz with isolation higher than 21 dB. Measured *S*-parameters show good agreement with simulated results. Orthogonal polarisation diversity has also been verified by calculating the difference between the θ and φ components of the *E*-field in selected planes. Finally, envelop correlation value below than −20 dB and group delay variations of <350 ps all over the operational band ensure that the proposed antenna system is well suited for portable UWB-MIMO applications.

7 References

1 Toh, W.K., Chen, Z.N., Xianming, Q., *et al.*: 'A planar UWB diversity antenna', *IEEE Trans. Antenna Propag.*, 2009, **57**, (11), pp. 3467–3473

2 Koohestani, M., Moreira, A.A., Skrivervik, A.K.: 'A novel compact CPW-fed polarization diversity ultrawideband antenna', *IEEE Antennas Wirel. Propag. Lett.*, 2014, **13**, pp. 563–566

3 Gallo, M., Daviu, E.A., Bataller, M.F., *et al.*: 'A broadband pattern diversity annular slot antenna', *IEEE Trans. Antennas Propag.*, 2012, **60**, (3), pp. 1596–1600

4 XIong, L., Gao, P.: 'Compact dual-polarized slot UWB antenna with CPW-fed structure'. Proc. of IEEE APS/URSI, 2012, pp. 1–2

5 Li, Y., Li, W.X., Liu, Ch., *et al.*: 'A printed diversity cantor set fractal antenna for ultra wideband communication applications'. Proc. of Antennas Propagation and EM Theory, 2012, pp. 34–38

6 Zhang, S., Ying, Z., Xiong, J., *et al.*: 'Ultrawide band MIMO/diversity antennas with a tree-like structure to enhance wideband isolation', *IEEE Antennas Wirel. Propag. Lett.*, 2009, **8**, pp. 1279–1282

7 Hong, S., Chung, K., Lee, J., *et al.*: 'Design of diversity antenna with stubs for UWB applications', *Microw. Opt. Technol. Lett.*, 2008, **50**, (5), pp. 1352–1356

8 Khan, M.S., Shafique, M.F., Capobianco, A.D., *et al.*: 'Compact UWB-MIMO antenna array with a novel decoupling structure'. Proc. 10th Int. Bhurban Conf. on Applied Sciences and Technology, 2013, pp. 347–350

9 See, T.S.P., Chen, Z.N.: 'An ultrawideband diversity antenna', *IEEE Trans. Antennas Propag.*, 2009, **57**, (6), pp. 1597–1605

10 Yoon, H.K., Yoon, Y.J., Kim, H., *et al.*: 'Flexible ultra wideband polarization diversity antenna with band-notched function', *IET Microw. Antennas Propag.*, 2011, **5**, (2), pp. 1463–1470

11 Lee, J.M., Kim, K.B., Ryu, H.K., *et al.*: 'A compact ultrawideband MIMO antenna with WLAN band-rejected operation for mobile devices', *IEEE Antennas Wirel. Propag. Lett.*, 2012, **11**, pp. 990–993

12 Liu, L., Cheung, S.W., Yuk, T.I.: 'Compact MIMO antenna for portable devices in UWB Applications', *IEEE Trans. Antennas Propag.*, 2013, **61**, (8), pp. 4257–4264

13 Adamiuk, G., Beer, S., Wiesback, W., *et al.*: 'Dual-orthogonal polarized antenna for UWB-IR technology', *IEEE Antennas Wirel. Propag. Lett.*, 2009, **8**, pp. 981–984

14 Lu, Y.C., Lin, Y.C.: 'A compact dual-polarized UWB antenna with high port isolation'. Proc. of IEEE Antennas Propagation Society International Symp. (APSURSI, 2010), Toronnto, ON, Canada, July 2010

15 Daviu, E.A., Gallo, M., Clemente, B.B., *et al.*: 'Ultrawideband slot ring antenna for diversity application', *Electron. Lett.*, 2010, **46**, (7), pp. 478–480

16 Zhang, S., Lau, B.K., Sunesson, A., *et al.*: 'Closely-packed UWB MIMO/diversity antenna with different patterns and polarizations for USB dongle application', *IEEE Trans. Antennas Propag.*, 2012, **60**, (9), pp. 4372–4380

17 Khan, M.S., Capobianco, A.D., Najam, A.I., *et al.*: 'Compact ultra-wideband diversity antenna with a floating parasitic digitated decoupling structure', *IET Microw. Antennas Propag.*, 2014, **8**, (10), pp. 743–753

18 Khan, M.S., Capobianco, A.D., Shafique, M.F., *et al.*: 'Isolation enhancement of a wideband MIMO antenna using floating parasitic elements', *Microw. Opt. Technol. Lett.*, 2015, **57**, (7), pp. 1677–1682

19 Tong, C., Guang-Ming, W., Jian-Gang, L., *et al.*: 'Application of ultra-compact single negative waveguide metamaterials for a low mutual coupling patch antenna array design', *Chin. Phys. Lett.*, 2014, **31**, (8), pp. 1–5

20 Ansoft High Frequency Structure Simulator (HFSS) Ver. 15.0: Ansoft Corporation. Available at http://www.ansoft.com., June 2014

21 Koohestani, M., Golpour, M.: 'U-shaped microstrip patch antenna with novel parasitic tuning stubs for ultra wideband applications', *IET Microw. Antennas Propag.*, 2010, **4**, (7), pp. 938–946